

## Article

# Gene editing of authentic *Brassica rapa* flavonol synthase 1 generates dihydroflavonol-accumulating Chinese cabbage

Sangkyu Park<sup>1,†</sup>, Hyo Lee<sup>1,†</sup>, Jaeun Song<sup>1</sup>, Chan Ju Lim<sup>2</sup>, Jinpyo Oh<sup>2</sup>, Sang Hoon Lee<sup>3</sup>, Saet Buyl Lee<sup>1</sup>, Jong-Yeol Lee<sup>1</sup>, Sunhyung Lim<sup>4</sup>, Jin A. Kim<sup>1</sup> and Beom-Gi Kim<sup>1,\*</sup>

<sup>1</sup>Metabolic Engineering Division, National Institute of Agricultural Sciences, Rural Development Administration, Jeonju, 54874, South Korea

<sup>2</sup>Institute of Biotechnology and Breeding, Asiaseed Inc., Icheon, 17414, South Korea

<sup>3</sup>Food and Nutrition Division, National Institute of Agricultural Sciences, Rural Development Administration, Wanju, 55365, South Korea

<sup>4</sup>Department of Horticultural Biotechnology, School of Biotechnology, Hankyong National University, Anseong, 17579, South Korea

\*Corresponding author. E-mail: bgkimpeace@gmail.com

<sup>†</sup>These authors contributed to this work equally.

## Abstract

Flavonols are the major class of flavonoids of green Chinese cabbage (*Brassica rapa* subsp. *pekinensis*). The *B. rapa* genome harbors seven flavonol synthase genes (*BrFLSs*), but they have not been functionally characterized. Here, transcriptome analysis showed four *BrFLSs* mainly expressed in Chinese cabbage. Among them, only *BrFLS1* showed major FLS activity and additional flavanone 3 $\beta$ -hydroxylase (F3H) activity, while *BrFLS2* and *BrFLS3.1* exhibited only marginal F3H activities. We generated *BrFLS1*-knockout (*BrFLS1*-KO) Chinese cabbages using CRISPR/Cas9-mediated genome editing and obtained transgene-free homozygous plants without off-target mutation in the T<sub>1</sub> generation, which were further advanced to the T<sub>2</sub> generation showing normal phenotype. UPLC-ESI-QTOF-MS analysis revealed that flavonol glycosides were dramatically decreased in the T<sub>2</sub> plants, while dihydroflavonol glycosides accumulated concomitantly to levels corresponding to the reduced levels of flavonols. Quantitative PCR analysis revealed that the early steps of phenylpropanoid and flavonoid biosynthetic pathway were upregulated in the *BrFLS1*-KO plants. In accordance, total phenolic contents were slightly enhanced in the *BrFLS1*-KO plants, which suggests a negative role of flavonols in phenylpropanoid and flavonoid biosynthesis in Chinese cabbage. Phenotypic surveys revealed that the *BrFLS1*-KO Chinese cabbages showed normal head formation and reproductive phenotypes, but subtle morphological changes in their heads were observed. In addition, their seedlings were susceptible to osmotic stress compared to the controls, suggesting that flavonols play a positive role for osmotic stress tolerance in *B. rapa* seedling. In this study, we showed that CRISPR/Cas9-mediated *BrFLS1*-KO successfully generated a valuable breeding resource of Chinese cabbage with distinctive metabolic traits and that CRISPR/Cas9 can be efficiently applied in functional Chinese cabbage breeding.

## Introduction

Flavonoids are important bioactive compounds naturally found in the plant kingdom. Therefore, the flavonoid biosynthesis pathway has been thoroughly investigated in various plant species. The first step in flavonoid biosynthesis involves condensation of *p*-Coumaroyl-CoA with three molecules of malonyl-CoA to produce chalcone, which is catalyzed by chalcone synthase (CHS). Chalcone is then subjected to intramolecular cyclization to form (2S)-flavanone by chalcone isomerase (CHI); (2S)-flavanone serves as a universal substrate for flavonoid biosynthesis, which is hydroxylated by flavanone 3 $\beta$ -hydroxylase (F3H) to form dihydroflavonols, which are further oxidized to flavonols by flavonol synthase (FLS). Dihydroflavonols can also be consecutively converted to form the anthocyanin precursors leucoanthocyanidins and anthocyanidins by dihydroflavonol 4-reductase (DFR) and anthocyanidin synthase (ANS), respectively. In another branch, (2S)-flavanone is converted to flavones by flavone synthase I or II (FNSI or FNSII).

Chinese cabbage (*Brassica rapa* var. *pekinensis*), widely cultivated in East Asia, is an economically important crop. Particularly,

green heading Chinese cabbages are consumed as the main ingredient of kimchi. Green Chinese cabbage contains various bioactive molecules, e.g. carotenoids, glucosinolates, and phenolic compounds. Among them, phenolic compounds that exhibit characteristic antioxidants account for a large proportion. The major classes of phenolic compounds accumulating in green Chinese cabbage are flavonoids, mainly flavonols, and phenolic acids [1, 2]. In Brassicaceae, *Arabidopsis thaliana* FLS (*AtFLS*) and *Brassica napus* FLS (*BnaFLS*) families have been functionally characterized. *Arabidopsis thaliana* genome harbors six *AtFLSs* on chromosome 5, among which *AtFLS1* encodes the major active FLS enzyme [3], and *AtFLS3* marginally contributes to flavonol biosynthesis [4]. In *B. napus*, 13 candidate FLS genes were identified, among which *BnaFLS1-1* and *BnaFLS1-2* are known as mainly active isoforms, and *BnaFLS3-3* and *BnaFLS3-4* encode enzymes marginally exhibiting F3H activity, whereas the other members of this family were proposed to be pseudogenes [5]. *Brassica rapa*, which diverged from *A. thaliana*, has undergone tandem duplications, whole-genome triplication, polyploidization, and fractionation of its subgenomes. Consequently, homologs of *B. rapa* FLS (*BrFLS*) genes

Received: 11 September 2023; Accepted: 6 November 2023; Published: 14 November 2023; Corrected and Typeset: 5 December 2023

© The Author(s) 2023. Published by Oxford University Press on behalf of Nanjing Agricultural University. This is an Open Access article distributed under the terms of the Creative Commons Attribution License (<https://creativecommons.org/licenses/by/4.0/>), which permits unrestricted reuse, distribution, and reproduction in any medium, provided the original work is properly cited.

are distributed across four different chromosomes (A02, A06, A09, and A10) [6–8]. Six *BrFLS* homologs, *BrFLS1*, *BrFLS2*, *BrFLS3.1*, *BrFLS3.2*, *BrFLS3.3*, and *BrFLS4.1*, were suggested to be syntenic orthologs of four *AtFLS* genes, *AtFLS1*, *AtFLS2*, *AtFLS3*, and *AtFLS4*, respectively, but those corresponding to *AtFLS5* and *AtFLS6* are absent from the *B. rapa* genome [7]. An additional *FLS* gene (named *BrFLS4.2* in this study) was recently assigned to belong to the *FLS4* group, although its syntenic relationship has not been investigated [5]. Therefore, a total of seven *BrFLS* homologous genes have been assigned. Among them, *BrFLS1* (Bra009358), a syntenic ortholog of *AtFLS1*, was predicted to encode a functional *FLS* enzyme, since *BrFLS1* expression was predominantly higher among other homologs but was not correlated with expression of *BrDFR* genes or anthocyanin accumulation in purple Chinese cabbage [9]. However, the functional differences between the seven *BrFLS* homologs have not been revealed, and the key *FLS* gene mainly responsible for flavonol biosynthesis in *B. rapa* has yet to be determined.

Clustered regularly interspaced short palindromic repeats (CRISPR)/CRISPR-associated (Cas) technology-mediated genome editing (GE) has been used to edit DNA sequences in numerous species due to its simplicity, high efficiency, versatility, and capacity for multiplexing [10]. Since 2015, >45 applications of CRISPR/Cas-mediated GE have been reported in Brassicaceae crops. Most were conducted in *Brassica oleracea* or *B. napus* to improve commercially important agronomic traits or nutritional values such as seed oil, carotenoids, or glucosinolate contents. Most of these studies used CRISPR/CRISPR-associated protein 9 (Cas9) to generate insertions/deletions (InDels) in single or multiple genes [11]. Only a few studies have reported modifying genes using CRISPR/Cas9 in *B. rapa*. These studies focused on genes involved in flowering time [12], leaf color transition [13], methylation of pectin [14], self-incompatibility [15], and circadian rhythms [16]. However, considering that the end goal of CRISPR/Cas9 GE is to obtain a transgene-free homozygous plant harboring a precise modification of a specific target gene, and the altered sequence and the resulting traits should be stably inherited, there is still a need for efficiency improvement and diversification of objectives in the CRISPR/Cas9 application for *B. rapa*.

Here, comparative analyses of gene expression and enzyme activities of the *BrFLS* homologs characterized the *BrFLS* family genes and indicated that *BrFLS1* is the only candidate for the major active *FLS* gene in *B. rapa*. The CRISPR/Cas9 targeting *BrFLS1* was introduced to a commercial inbred line of green Chinese cabbage to generate *BrFLS1*-knockout (*brfls1*) plants, and we obtained transgene-free homozygous *brfls1* lines in the T<sub>1</sub> generation. Flavonol glycosides, the major class of flavonoids in the background variety, dramatically decreased, and instead dihydroflavonol glycosides accumulated in the *brfls1* lines. We showed an effective way of metabolic engineering to develop new varieties of Chinese cabbage with modified flavonoid profiles using CRISPR/Cas9 GE system. Furthermore, our study provides insights into understanding the phenylpropanoid and flavonoid biosynthetic pathway in *B. rapa*.

## Results

### Comparative analysis of gene expression and amino acid sequences of *BrFLS* homologs

We estimated the expression levels of each *BrFLS* homolog in the leaves of two 9- and 42-day-old green Chinese cabbage varieties, 5546 and 5923, using transcriptome deep sequencing (RNA-seq). Among the seven *BrFLS* genes, *BrFLS1*, *BrFLS2*, *BrFLS3.1*, and

*BrFLS4.2* were mainly expressed in all three varieties. In particular, *BrFLS1* and *BrFLS2* showed substantially higher expression levels than the other homologs (Fig. 1A & Supplementary Table S2). The four genes were further investigated for their characterization. According to our pretest, varieties 5546 and 5923 showed very low transformation efficiencies, thus we used another green variety, 8045, which showed high transformation efficiency, as the target variety for further analysis. First, we isolated the CDSs of *BrFLS1*, *BrFLS2*, *BrFLS3.1*, and *BrFLS4.2* from the cauline leaves of variety 8045. Sequencing analysis revealed that the *BrFLS1* CDS differs by 10 nucleotides from the reference sequence (Bra009358) (Supplementary Data Fig. S1), resulting in four amino acid substitutions (T40V, A57E, K83Q, and N313Y) (Fig. 1B), and the *BrFLS3.1* CDS had two nucleotide changes compared to the reference sequence (Bra038648) (Supplementary Data Fig. S2) resulting in one amino acid substitution (K261E) (Fig. 1B), whereas the *BrFLS2* and *BrFLS4.2* coding sequences isolated from the variety 8045 were identical to the reference sequences (Bra038647 and Bra018076, respectively). We aligned the deduced amino acid sequences of the seven *BrFLS* homologs along with *AtFLS1*, *ZmFLS1* in maize (*Zea mays*), *BnaFLS3–3*, and three F3Hs including *AtF3H*, *GmF3H* in soybean (*Glycine max*), and *OsF3H* in rice (*Oryza sativa*). All sequences have completely conserved core motifs of 2-ODD, such as ferrous ion binding (HxDxNH) and 2-oxoglutarate binding (Rxs) motifs [17], but, in other areas, FLSs and F3Hs were clearly distinguished. Among FLSs, only *AtFLS1* and *BrFLS1* (*BrFLS1*/8045) completely share the three FLS-specific 'PxxxIRxxxEQP', 'CPQ/RPxLAL', and 'SxxTxLVP' motifs [18], and *ZmFLS1* has the three motifs with partial or complete conservations. *BrFLS1* shared 91.4% identity with *AtFLS1*, whereas the other homologs showed ~60%–67% identity with *AtFLS1*. These analyses suggest that, among the *BrFLS* homologs, only *BrFLS1* has a complete structure. Notably, *BrFLS1* and *BrFLS3.1* had conserved residues at the positions proposed to be involved in substrate binding and proper protein folding [19], whereas *BrFLS2* and *BrFLS4.2* had variations at these positions (Fig. 1B).

### Recombinant *BrFLS1* protein is a bifunctional enzyme exhibiting both FLS and F3H activities

Substrate-feeding assays were performed to characterize the enzymatic properties of recombinant GST-fused *BrFLS1*, *BrFLS2*, *BrFLS3.1*, and *BrFLS4.2* with different substrates, DHK or Nar. SDS-PAGE analysis showed the successful production of all recombinant GST-fused proteins upon IPTG induction (Fig. 2A). HPLC analysis of DHK-fed reactants showed that only *BrFLS1* produces a large amount of kaempferol (K) from DHK. However, K was almost absent in the reactants of *BrFLS2*, *BrFLS3.1*, and *BrFLS4.2* (Fig. 2B, left panel). K-like small peaks were shown in the reactants of *BrFLS2*, *BrFLS3.1*, and *BrFLS4.2*, but the same peak at a similar level was detected in the vector control (VC), indicating that these peaks are not specific products by the *BrFLS*s. Therefore, *BrFLS1* was the only enzyme with FLS activity among the four *BrFLS*s tested. Next, we tested if the *BrFLS*s also have F3H activity via a Nar feeding as a substrate. We detected DHK and K simultaneously in the Nar-fed reactant of *BrFLS1* (Fig. 2B, right panel), indicating that Nar was converted to DHK by the F3H activity of *BrFLS1* and then converted to K by its FLS activity, which suggests that *BrFLS1* is a bifunctional enzyme with both F3H and FLS activities. At a narrowed range of absorbance, we observed trace levels of DHK in the reactants of *BrFLS2* and *BrFLS3.1*, but not of *BrFLS4.2*, indicating that *BrFLS2* and *BrFLS3.1* lack FLS activity but only have faint levels of F3H activity. The conversion rate of each reaction was calculated (Fig. 2C), which

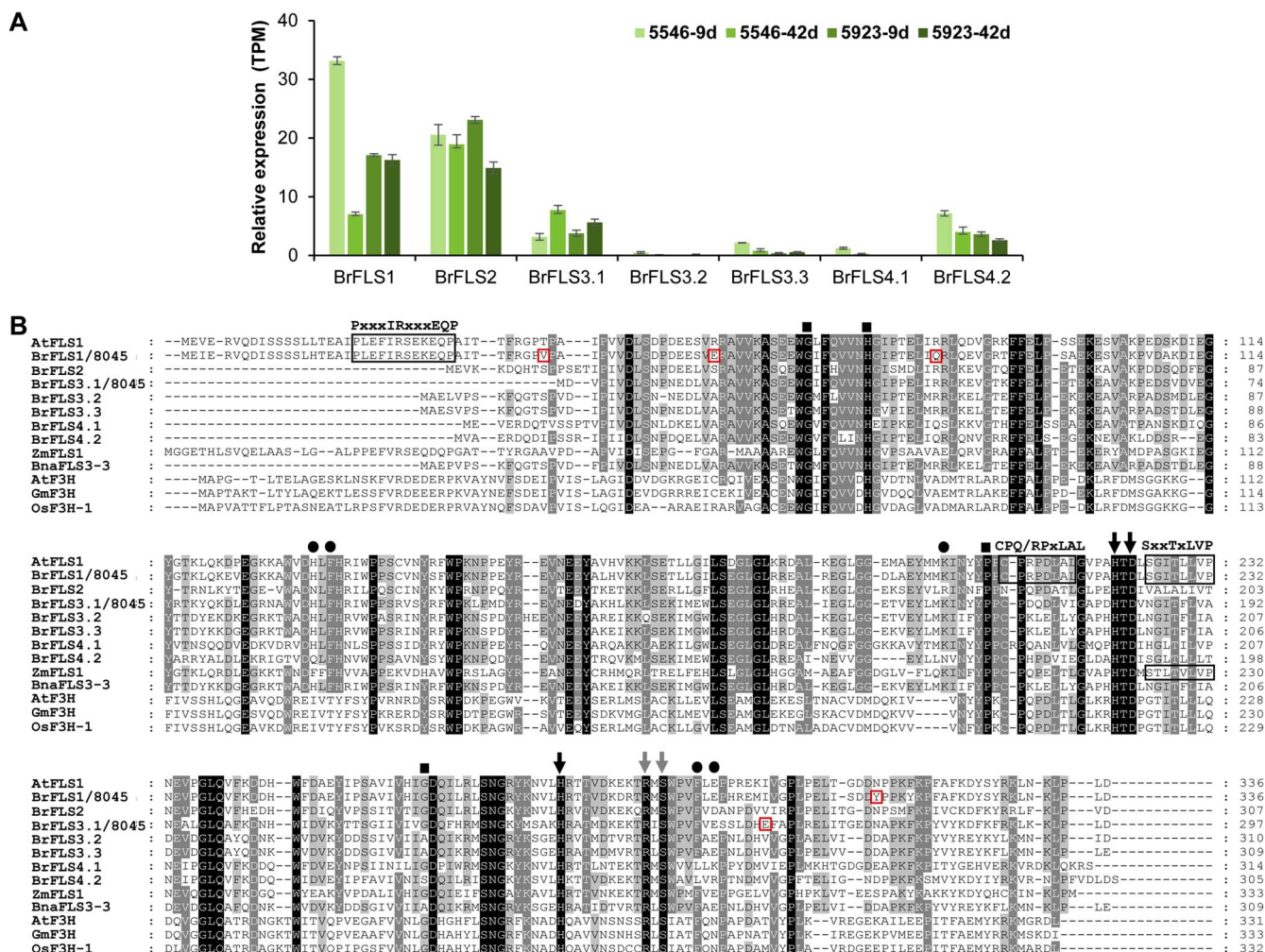


**Figure 1.** Comparative analysis of gene expression and amino acid sequences of BrFLS homologs. (A) Relative gene expression levels of BrFLS homologs based on mRNA-TPM (transcript per million) from the RNA-seq analysis of leaves from 9- and 42-day-old plants of 5546 and 5923 varieties. Error bars indicate  $\pm$  SD from three replicates. (B) Alignment was conducted using the ClustalW program. Identical amino acids are indicated with black backgrounds. Amino acids that are  $>80\%$  conserved are indicated with dark grey backgrounds, and those that are  $>60\%$  conserved are indicated with light grey backgrounds. Three boxes represent FLS-specific motifs 'PxxxIRxxxEQP', 'CPQ/RPxLAL', and 'SxxTxLVP'. Amino acid residues responsible for binding ferrous iron and 2-oxoglutarate are marked with black and grey arrows, respectively. Predicted residues involved in substrate binding are marked with black circles. Functional residues suggested to be involved in proper folding of the FLS polypeptide are marked with black squares. Amino acid variations of BrFLS1 and BrFLS3.1 that were cloned from variety 8045 are indicated by red rectangles.

showed that BrFLS1 had a conversion rate of  $60.5 \pm 4.3\%$  for FLS activity and  $47.5 \pm 3.6\%$  for F3H activity, but the conversion rates of BrFLS2 and BrFLS3.1 for F3H activity were approximately 100-fold lower ( $0.41 \pm 0.05\%$  and  $0.55 \pm 0.06\%$ , respectively) than that of BrFLS1, suggesting that BrFLS1 is the authentic FLS enzyme with additional F3H activity, and BrFLS2 and BrFLS3.1 can only marginally contribute to dihydroflavonol biosynthesis in *B. rapa*. The bifunctional activity of BrFLS1 was verified by agroinfiltration of *N. benthamiana* leaves (Supplementary Data Fig. S3). Additionally, we supplied the same concentration of DHK or DHQ into the infiltrated leaves and compared the K and quercetin (Q) products. The result showed that K production was  $\sim 2.5$ -fold higher than Q production (Supplementary Data Fig. S4), suggesting a substrate preference biased toward DHK over DHQ.

## Generation of transgene-free homozygous *brfls1* plants

We generated BrFLS1-knockout Chinese cabbage using CRISPR/Cas9. To induce an InDel mutation leading to a frameshift in the BrFLS1 coding region, we designed three sgRNAs (sg1, sg2, and

sg3) targeting specific sequences on the first exon of BrFLS1. Each sgRNA was introduced into the binary vector pHatC harboring a 35S promoter-driven *Streptococcus pyogenes* Cas9 (*SpCas9*) expression cassette (Fig. 3A) [20] and applied for *Agrobacterium*-mediated transformation of variety 8045. We obtained four T<sub>0</sub> plants (NB60, 61, 62, and NB63) from the sg3-transformed calli. The transformation efficiency was  $\sim 1.2\%$  (four T<sub>0</sub> plants/336 explants). Targeted deep-sequencing analysis revealed that the T<sub>0</sub> plants that harbored single A or T insertions mainly occurred 3 bp upstream of the PAM sequence in their BrFLS1 sequences. The editing efficiencies of T<sub>0</sub> plants were 81.6% in NB60, 11.3% in NB61, 99.8% in NB62, and 0.2% in NB63. We tried to get transgene-free homozygous lines in the T<sub>1</sub> generation. We obtained the transgene-free T<sub>1</sub> plants in NB61 and NB62 with 58.7% and 3.5% probabilities, respectively. However, we were able to get transgene-free homozygous BrFLS1-knockout T<sub>1</sub> plants from only NB62 (NB62-180, -203, and -204), and they were referred to as *brfls1* (Supplementary Table S3). We performed off-target analyses on four predicted off-target sequences similar to the sg3 target sites and the corresponding sequences in the six other BrFLS homologs,

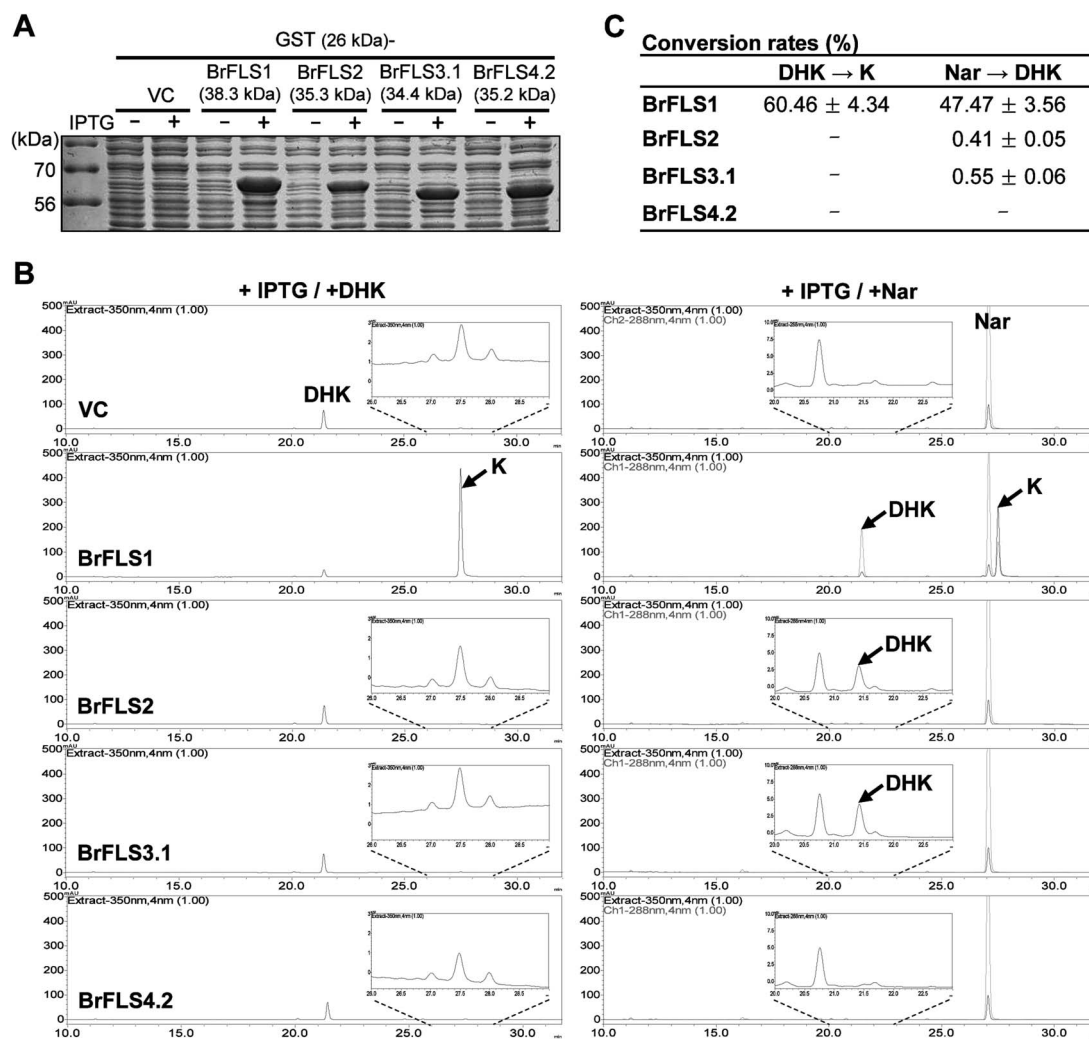


**Figure 2.** Substrate-feeding assays of recombinant BrFLS homologs. (A) GST-fused BrFLS1, BrFLS2, BrFLS3.1, and BrFLS4.2 were expressed in *E. coli* by IPTG induction, which was verified by SDS-PAGE. VC, vector control. (B) IPTG-induced bacterial cultures were fed with DHK or Nar as a substrate. HPLC identified K production from DHK-fed reactant and DHK and K production from Nar-fed reactant. Nar and DHK were identified at 288 nm (grey chromatogram), and K was identified at 350 nm (black chromatogram). Small peaks of K and DHK are enlarged and shown in the insets. (C) Conversion rates were calculated based on the molar ratio between input and consumed substrates. The mean values were determined from three replicates.

which identified no mutations in the sequences in the three *brfls1* T<sub>1</sub> plants (Supplementary Table S4). T<sub>2</sub> progenies of the *brfls1* plants were generated and cultivated in the greenhouse to form head together with the variety 8045 and non-edited T<sub>2</sub> progenies of NB61–99 as controls (Fig. 3B). Genomic PCR and sequencing analysis verified that the A or T insertion in the target site resulting in the C-terminal truncation of BrFLS1 (Fig. 3C and 3D) and the absence of the transgene (Fig. 3E) were successfully inherited in the *brfls1* T<sub>2</sub> progenies.

### Significant reduction of flavonols and concomitant accumulation of dihydroflavonols in the *brfls1* T<sub>2</sub> plants

To investigate whether the flavonoid content and profile changed, we sampled leaves from the middle layers of the cabbage head from four *brfls1* T<sub>2</sub> individuals of each line and performed liquid chromatography and electrospray ionization quadrupole time-of-flight mass spectrometry (LC-ESI-QTOF-MS) with negative ionization mode. Flavonoid aglycones were extracted from the lyophilized leaves with acid hydrolysis and analyzed along with K, Q, DHK, and DHQ aglycones as

standards. The extracted ion chromatograms (XICs) showed significant reduction of K ( $m/z$  285.23 [M-H]<sup>-</sup>) and Q ( $m/z$  301.23 [M-H]<sup>-</sup>) in the *brfls1* lines. Approximately 93%–97% (84–87 nmole·g<sup>-1</sup> FW) of K and 57%–82% (20–28 nmole·g<sup>-1</sup> FW) of Q were reduced in the *brfls1* T<sub>2</sub> progenies compared to the NB61–99 progenies. On the other hand, DHK ( $m/z$  287.25 [M-H]<sup>-</sup>) and DHQ ( $m/z$  303.25 [M-H]<sup>-</sup>) that are absent in the NB61–99 progenies accumulated in the *brfls1* T<sub>2</sub> progenies (Fig. 4A) to ~71–88 nmole·g<sup>-1</sup> FW and 8–13 nmole·g<sup>-1</sup> FW, respectively, which are comparable to the reduced levels of K and Q. However, isorhamnetin (IR:  $m/z$  315.26 [M-H]<sup>-</sup>) contents were not significantly changed and cyanidin (Cya:  $m/z$  286.24 [M-H]<sup>-</sup>) was absent in the *brfls1* plants. These results indicate that blocking flavonol biosynthesis resulted in accumulation of its dihydroflavonol precursors in green Chinese cabbage. Furthermore, LC-ESI-QTOF-MS/MS analysis of 70% (v/v) methanol extracts of the leaves identified dihydroflavonol glycosides accumulated in the *brfls1*, which showed four and three major peaks corresponding to DHK and DHQ glycosides, respectively, in the *brfls1* T<sub>2</sub> plants. According to their MS/MS spectra, they were tentatively assigned as three different

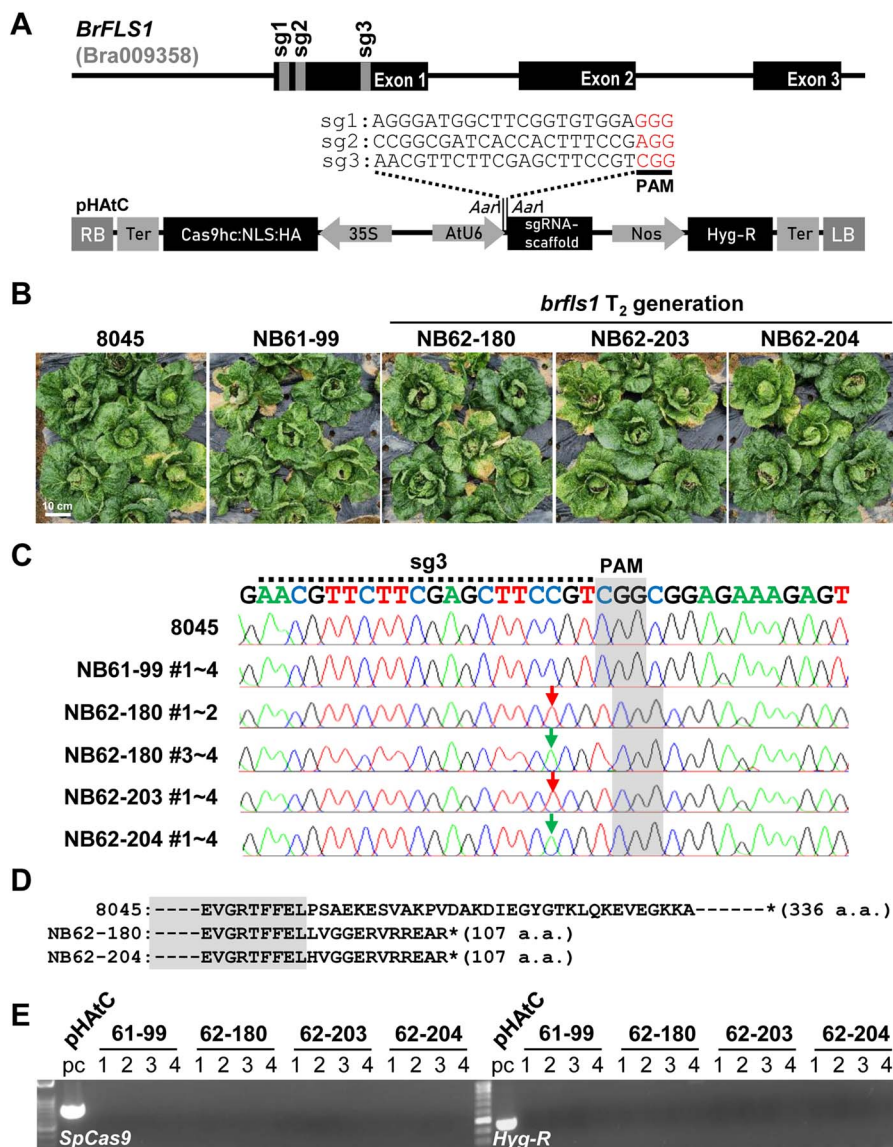


**Figure 3.** Generation of transgene-free homozygous *brfls1* plants. (A) Diagram of binary vector construction. Three sgRNAs (sg1, sg2, and sg3) were selected in exon 1 of the *BrFLS1* gene and were introduced into the binary vector *pHAtC* carrying *SpCas9*, sgRNA scaffold, and the hygromycin resistance gene (*Hyg-R*). (B) T<sub>2</sub> progenies of *brfls1* plants (NB62-180, -203, and -204) and control plants (8045 and T<sub>2</sub> progenies of NB61-99) grown in green house. (C) The regions encompassing the *sg3* target site (dashed line) were amplified by genomic PCR and sequenced, which showed single T (red arrow) or A (green arrow) insertion 3 bp upstream of the PAM sequence (5'-CGG-3') (shaded grey) in the target site of *BrFLS1* in the *brfls1* T<sub>2</sub> plants. (D) Deduced amino acid sequences of the *brfls1* harboring the T or A insertion show early stops of *BrFLS1* translation after 107<sup>th</sup> amino acid caused by a frameshift. (E) Genomic PCR of four individuals (1-4) of the *brfls1* T<sub>2</sub> progenies showing absence of transgene in their genome.

DHK-hexosides and one DHQ-dihexoside and two different DHQ-hexosides, respectively (Fig. 4C and Supplementary Data Fig. S5). Although the presence of other minor contributors in flavonol biosynthesis cannot be ruled out, these results clearly show that *BrFLS1* is the major active FLS enzyme in Chinese cabbage.

### Upregulation of the phenylpropanoid and flavonoid biosynthetic genes caused slight increases in total phenolics in the *brfls1* T<sub>2</sub> plants

To explore whether the change in the flavonoid profile caused by knocking out *BrFLS1* was accompanied by changes in the expression patterns of phenylpropanoid and flavonoid biosynthetic genes, we performed qPCR analysis with total RNA isolated from the T<sub>2</sub> plants of *brfls1* and NB61-99. The early step of phenylpropanoid and flavonoid biosynthesis, such as

*BrPALs* (*BrPAL1.2*, *BrPAL2.1*, *BrPAL2.3*, and *BrPAL3.2*), *BrC4H1* and *BrCHSs* (*BrCHS1* and *BrCHS3*), and *BrF3'H* that is responsible for flavonoid B-ring hydroxylation were remarkably upregulated in the *brfls1* plants. These results suggest that metabolic flux into the lignin branch or flavonoid branch can be enhanced by blocking *BrFLS1*. Thus, we examined whether levels of total phenolics were changed in the *brfls1* plants, and we found that the total phenolic contents slightly but significantly increased to ~13% in the *brfls1* plants compared to the control plants (Fig. 5).

### Phenotypic changes of the *brfls1* plants

We surveyed the agronomic traits of *brfls1* T<sub>2</sub> Chinese cabbage, indicating that their heads were somewhat lighter than the controls, and although there were individual variations, tip burn symptoms were observed in the middle layers of the

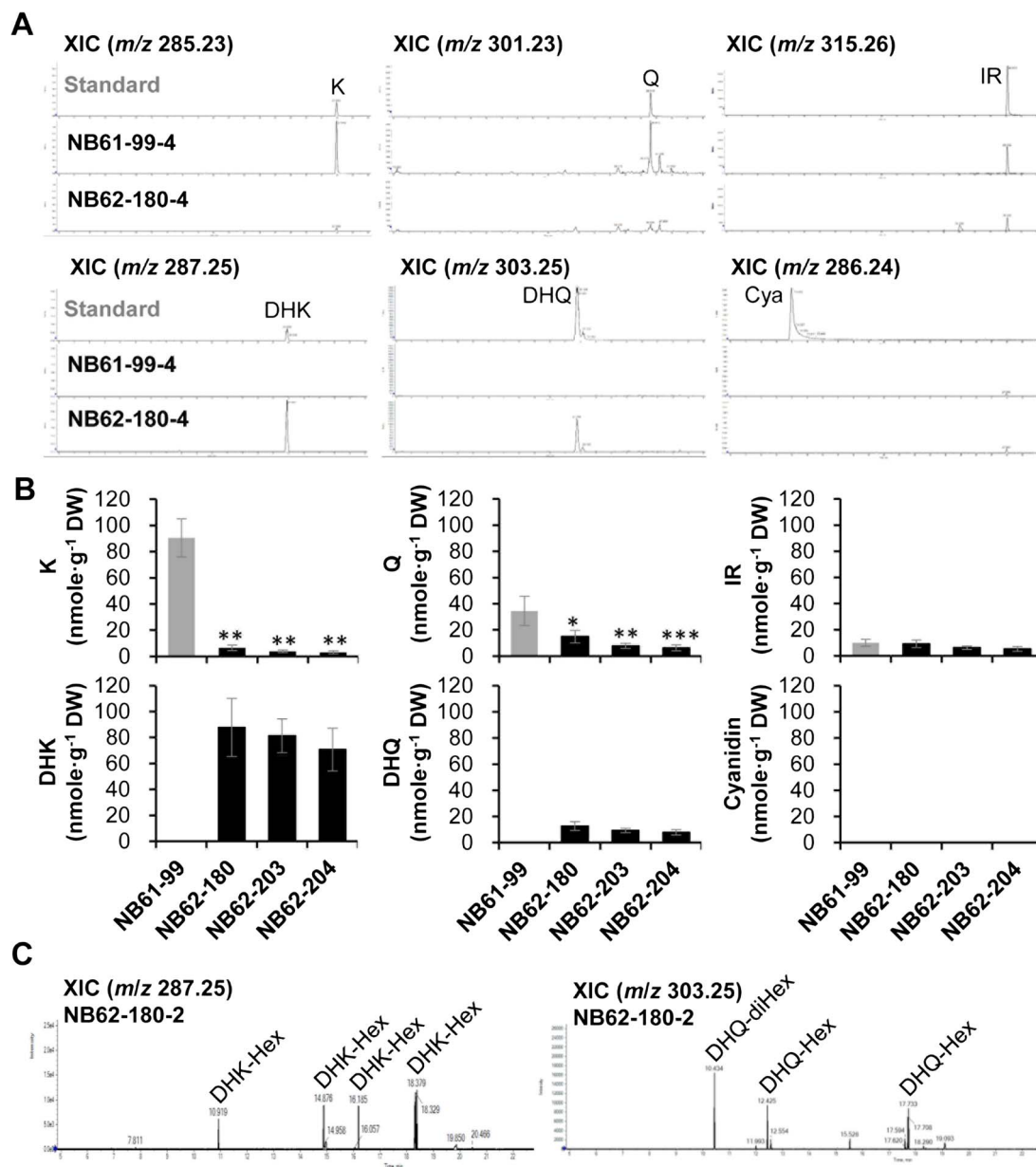


**Figure 4.** Investigation of changes in the flavonoid profile of *brfls1* plants using LC-ESI-QTOF-MS analysis. LC-ESI-QTOF-MS analysis of flavonoid aglycones extracted from the leaves of four  $T_2$  individuals generated from the NB61-99 (WT) and *brfls1* (NB62-180, NB62-203, NB62-204) with negative ionization mode. (A) Representative XICs displaying mass spectra of flavonoid aglycones in the  $T_2$  plants. XICs at  $m/z$  285.23,  $m/z$  287.25,  $m/z$  301.23,  $m/z$  303.25,  $m/z$  315.26, and  $m/z$  286.24 show deprotonated K, DHK, Q, DHQ, IR, and cyanidin Cya aglycones, respectively. (B) The average values of flavonoid content in the four individuals of each  $T_2$  line were calculated based on the areas of corresponding standards. The mean values  $\pm$  SD of four independent biological samples are shown. Significant differences were determined by Student's *t*-tests. Asterisks indicate significant differences from the WT (\* $P$  < 0.05, \*\* $P$  < 0.01, \*\*\* $P$  < 0.001). (C) Representative XICs of dihydroflavonol glycosides extracted from the *brfls1*  $T_2$  plants using 70% methanol (Hex, hexoside; diHex, dihexoside).

*brfls1* heads. Their shape tended to be vertically elongated due to the increased mid-vein lengths compared to the controls (Fig. 6A and 6B). In terms of reproductive phenotypes, there were no significant differences in bolting, flowering, seed color, and seed weight between *brfls1* and the controls (Supplementary Data Fig. S6). However, root lengths and chlorophyll contents of *brfls1* seedlings were reduced slightly but significantly by a plethora of mannitol (200 mM or 400 mM), but not of NaCl (150 mM), compared to those of the controls (Fig. 6C, 6D, Supplementary Data Fig. S7, and S8), suggesting that flavonols play a positive role in osmotic stress tolerance during early growth of Chinese cabbage.

## Discussion

In the Brassicaceae lineage, integrative studies on *FLS* family genes were previously carried out in *A. thaliana* [3, 18] and *B. napus* [5], providing important references for understanding the characteristics of the *BrFLS* family. The expression of *FLS1s*, *FLS2s*, and *FLS3s* was commonly observed in *A. thaliana*, *B. napus*, and *B. rapa*; however, the expression patterns of each group are species-specific. *FLS1s* are predominantly expressed in all three species, whereas *FLS2s* are expressed at high levels in *A. thaliana* and *B. rapa* but at marginal levels in *B. napus*. *FLS3s* are expressed at minor levels in all three species except for *BnaFLS3-3* and *BnaFLS3-4*, which are highly expressed in *B. napus*. Interestingly,

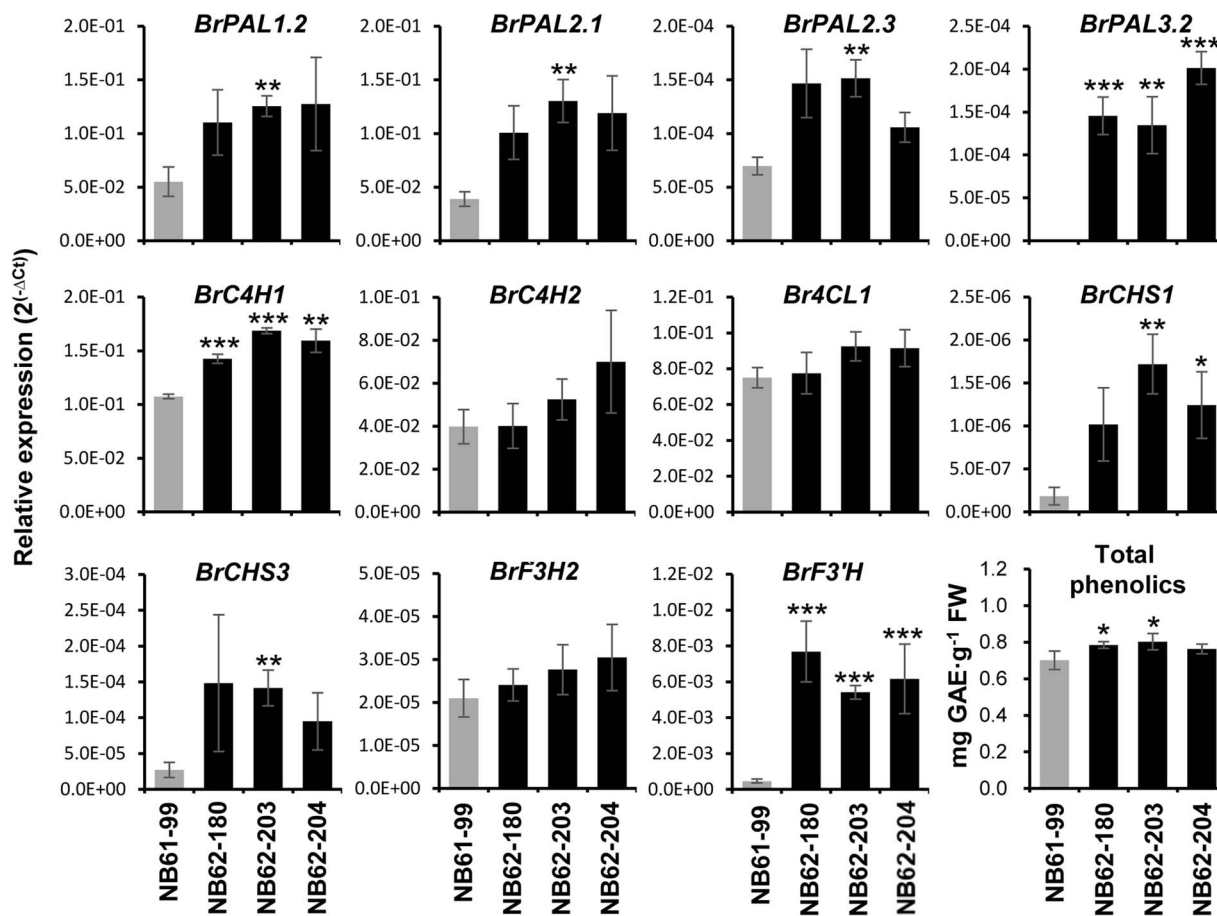


**Figure 5.** Analyses of changes in the expression of flavonoid biosynthetic genes and total phenolic contents in the *brfls1* T<sub>2</sub> plants. qPCR analysis was performed and total phenolic content was measured in the four T<sub>2</sub> individuals generated from the NB61-99 and *brfls1* (NB62-180, NB62-203, NB62-204). Expression values were normalized using *B. rapa* Actin7 (*BrACT7*) transcript. The total phenolic contents were calculated using gallic acid as a standard, and the mean values were expressed as milligrams of gallic acid equivalents per gram of fresh weight (mg GAE·g<sup>-1</sup> FW). The mean values  $\pm$  SD of four independent biological samples are shown. Significant differences were determined by Student's t-tests. Asterisks indicate significant differences from the WT (\**P* < 0.05, \*\**P* < 0.01, \*\*\**P* < 0.001).

nonfunctional *AtFLS2*, a pseudogene encoding a protein lacking the key C-terminal [18], was inherited as a functional *BrFLS2* exhibiting F3H activity in *B. rapa*. Furthermore, the *BrFLS2* was inherited in *B. napus* as nonfunctional *BnaFLS2s* pseudogenized again [5]. In the case of the *FLS3s*, *AtFLS3*, exhibiting only marginal FLS activity, was inherited in *B. rapa* as *BrFLS3.1* exhibiting F3H activity, but afterward, *BrFLS3.1* has been inherited in *B. napus* as *BnaFLS3-1* and *BnaFLS3-2* almost pseudogenized. Moreover, the *BnaFLS3-3* and *BnaFLS3-4* exhibiting F3H activity were derived from *BrFLS3-2* and *BrFLS3-3*, which were shown not to be expressed (seemed to be almost pseudogenized) in this study. The dynamic history of Brassicaceae FLS evolution implies that flavonoid biosynthesis has been enhanced during evolution of Brassica species.

Comparing the deduced amino acid sequences of the seven *BrFLSs* simply shows that only *BrFLS1* encodes complete structure for authentic FLS in the *B. rapa* genome. The substrate-feeding assays of *BrFLS1* showed that its F3H and FLS activities were nearly comparable, suggesting that *BrFLS1* contributes to dihydroflavonol production at a substantial level along with *BrF3H* in Chinese cabbage. Even though the amino acid sequences of *BrFLS2* and *BrFLS3.1* are distinct from those of *BrF3Hs*, they were shown to have only F3H activity but not FLS activity (Fig. 2) like *BnaFLS3.3* and *BnaFLS3.4* [5], which indicates that

the 'PxxxIPxxxEQP' motif is unnecessary for their F3H activities. However, considering that Maize (*Z. mays*) *ZmFLS1*, exhibiting only FLS activity [21], has partially matching 'PxxxIPxxxEQP' and 'CPQ/RPxLAL' motifs and a completely conserved SxxTxLVP motif, the existence of the three motifs itself is likely to be essential for FLS activity, regardless of whether it is FLS mono- or FLS/F3H bifunctional enzyme, and it can be further assumed that modest changes in these motifs can result in loss of F3H activity. The transient expression of *BrFLS1* in *N. benthamiana* leaves showed a substrate preference of *BrFLS1* biased towards DHK rather than DHQ. Likewise, *AtFLS1* prefers DHK to DHQ as a substrate, and its His-132 was proposed to be the residue responsible for the substrate preference [19]. *BrFLS1* also has an His-132 residue, which may account for its substrate preference for DHK.

Flavonoid analysis showed drastic decreases in flavonol glycosides and parallel accumulation of dihydroflavonol glycosides in the *brfls1* plants. To our knowledge, the accumulation of dihydroflavonol glycosides is the first reported in *B. rapa*. However, similar to the *A. thaliana* *FLS1* mutant (*atfls1*) [3], we observed residual flavonols in the *brfls1* plants. Considering our results of the sequence analysis and substrate-feeding assays, the source of the residual FLS activity was unlikely to come from the other *BrFLSs*. *AtANS* has been known as an alternative route for flavonol production in *A. thaliana*, and the *atans atfls1* double mutant

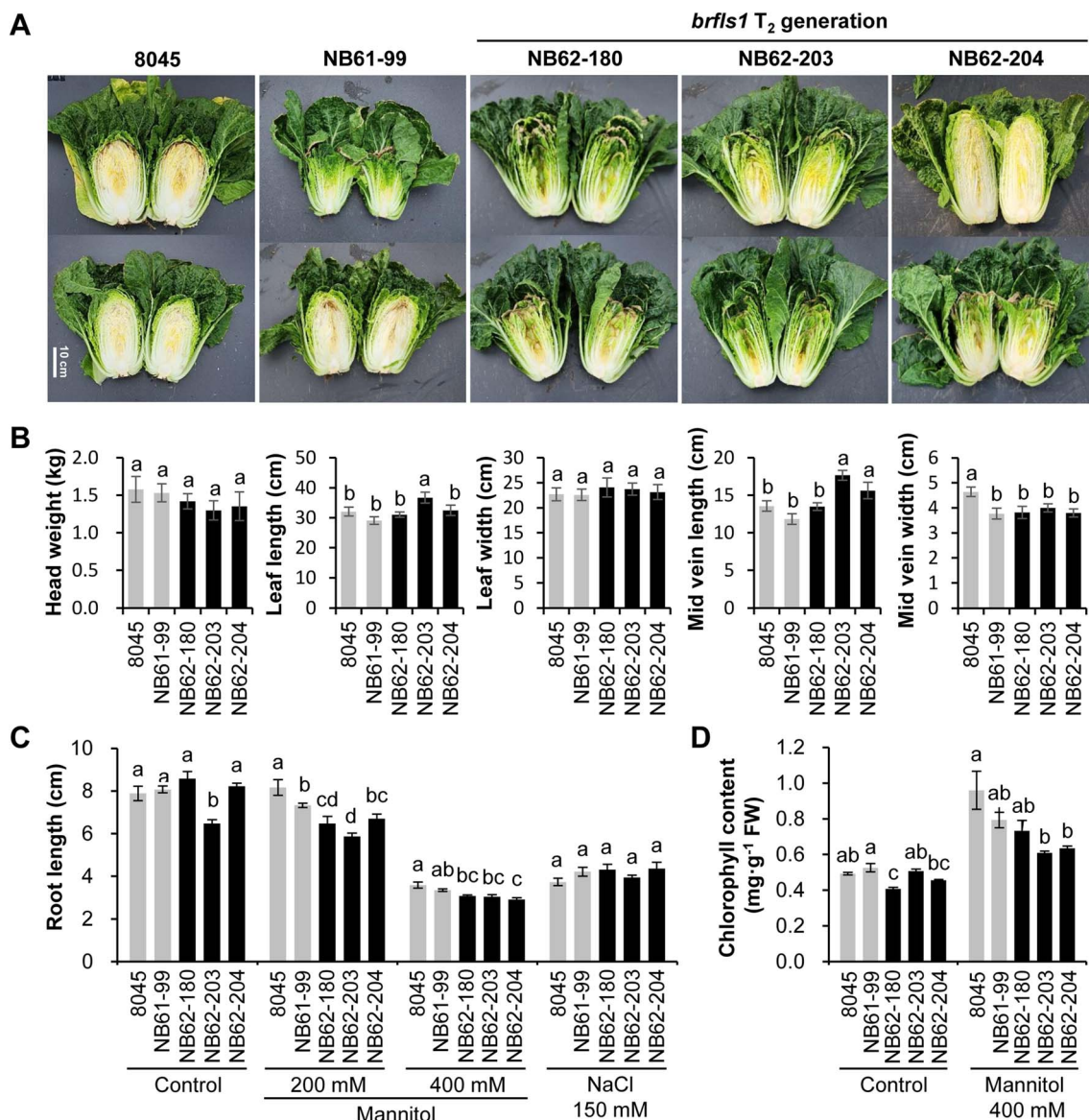


**Figure 6.** Phenotypic analyses of the *brfls1* T<sub>2</sub> plants. (A) Cross-sections of heads of two *brfls1* T<sub>2</sub> plants and controls (8045 and NB61-99). (B) Indices related to agricultural traits of their heads (C) Root lengths of seedlings of *brfls1* T<sub>2</sub> plants and control plants four (for control treatment) or six (for mannitol or NaCl treatment) days after osmolytes treatment. (D) Chlorophyll contents measured from aerial parts of the seedlings 4 days after mannitol treatment. The mean values  $\pm$  SD of four independent biological samples are shown. Statistical significance was determined by Duncan's Multiple Range Test using SAS (version 9.1) software. Significant differences between means ( $P < 0.05$ ) are indicated by different lower case letters (a, b, and c).

lacked most of the residual flavonols in *A. thaliana* [18], which supports the possibility that BrANS is a minor contributor in flavonol production in Chinese cabbage, although the expression levels of BrANSs in the *brfls1*, a green variety, is presumed to be very low [9]. The *atfls1* mutant shows drastic reduction of flavonol glycosides and parallel accumulation of anthocyanins as well as dihydroflavonol glycosides, which has been suggested to be due to activation of the late flavonoid biosynthesis genes (LBGs), e.g. *DFR*, *ANS*, and *UDP-glucose:flavonoid 3-O-glucosyltransferases* (*UGTs*), and *acyltransferases* (*ATs*) in association with flavonol-responsive regulators [18]. Unlike *atfls1*, the *brfls1* plants did not accumulate anthocyanins, which can be explained by the previous finding that green Chinese cabbages carry a defective *BrMYB2* allele containing a suppressive long intron, that makes green Chinese cabbage unable to produce anthocyanins [22]. The levels of decreased flavonols were nearly equivalent to the levels of accumulated

dihydroflavonols, implying that most of the metabolic flux converged into dihydroflavonols without leakage to the anthocyanin branch in the *brfls1* plants. Hence, if we focus on the special trait of Chinese cabbage accumulating dihydroflavonols, the genetic characteristics of green Chinese cabbage can be considered as a great advantage.

*BrPALs*, *BrC4H*, *BrCHSs*, and *BrF3'H* were upregulated in the *brfls1* plants, which suggests a possibility that flavonol itself can be involved in regulating the phenylpropanoid and flavonoid biosynthetic pathway in *B. rapa*. Similar patterns were reported in *atfls1*, in which *AtPAL1*, *AtPAL2*, *AtDFR*, and *AtANS* were upregulated [18, 23]. Importantly, flavonol aglycones, rising from compromised flavonol-3-O-conjugation in the *ugt78d1/ugt78d2* double mutant, led to feedback inhibition of phenylpropanoid and flavonoid biosynthetic genes, but the inhibitions were released in the *atchs ugt78d1 ugt78d2* triple mutant in which flavonol



production is completely blocked [23], which provides strong evidence that flavonol aglycones are important regulatory compounds in the phenylpropanoid and flavonoid biosynthetic pathway. Therefore, it can be speculated that the gene expression of *BrPALs*, *BrC4H*, *BrCHSs*, and *BrF3'H* in wild type is weakly inhibited by trace levels of flavonol aglycones, but in the *brfls1*, the opportunity for nascent free aglycones to be released is deprived by the drastic reduction of flavonol production and the resulting relatively excess capacity of UGT activity. Thereby, the inhibition at basal levels is released, resulting in upregulation of the genes in the *brfls1* plants. Indeed, LC-ESI-QTOF-MS analysis of NB61–99 showed trace amounts of flavonol aglycones (Supplementary Data Fig. S9).

The change in flavonoid profile seemed to negatively affect early growth of *brfls1*, suggesting the positive effect of flavonols on abiotic stress tolerance in Chinese cabbage. However, despite its vulnerability in stress at the seedling stage, it did not cause any disruption to growth under normal condition. As a result, the overall agricultural traits of *brfls1* Chinese cabbages, such as head formation and proliferation, are within the normal range, showing that their agricultural utility value is sufficient. But one thing to consider is whether abandoning the positive aspects of flavonols and replacing them with dihydroflavonols would have agricultural and dietary benefits. Flavonols are involved in various aspects of plant physiology as well as human health mainly due to their antioxidant properties. However, from an agricultural perspective, excessive accumulation of flavonols can detract from the commercial value of agricultural products. Insoluble flavonols may impair digestibility [24], and a kaempferol-glycoside causes the bitter taste of rapeseed (*B. napus* subsp. *napus*) protein isolate [25]. Accordingly, yellow-seeded *B. napus* varieties with reduced phenolics, e.g. epicatechin, isorhamnetin glucoside, and kaempferol glucosides, have been developed through interspecific hybridization ([26]; J. [27]). Therefore, the value of the *brfls1* plants needs to be considered in terms of dietary properties. The accumulation of dihydroflavonols is also of interest as various pharmaceutical properties of dihydroflavonols have been reported, such as anti-inflammation [28], improvement of insulin resistance [29], promotion of apoptosis [30], prevention of Alzheimer's disease [31], inhibition of T-cell activation [32], and protection of neuronal cells [33]. Although it is not clear to what extent these functionalities of dihydroflavonols are superior to those of flavonols, the *brfls1* Chinese cabbage lines could be considered as unique breeding resources to develop functional foods with improved bioactive or pharmaceutical properties.

## Materials and methods

### Plant materials and growth conditions

Seeds of three inbred lines of green Chinese cabbage (varieties 5546, 5923, and 8045) were provided by Asiaseed Inc. (Icheon, South Korea). Nine-day-old seedlings, grown on Murashige and Skoog (MS) medium, were further grown in soil for 42 days under 16-h/8-h light/dark condition at 25°C. Cauline leaves of the 9- and 42-day-old plants were harvested for total RNA extraction. To induce flowering and silique formation, young seedlings grown on soil for ~2 weeks were vernalized for ~6 weeks.

### Total RNA extraction and RNA sequencing analysis

Cauline leaves of the 9- and 42-day-old plants were used for total RNA extraction using a FavorPrep Plant Total RNA Mini Kit (Favorgen, Pingtung, Taiwan, China). RNA samples were sent to

Theragen Bio Corp. (Gyeonggi Province, Republic of Korea) for RNA sequencing with an Illumina HiSeq 4000 system (Illumina, San Diego, CA, USA). The sequence quality of raw reads was evaluated with FastQC (version 0.11.9). High-quality reads were aligned to reference genome of Chinese cabbage (<http://brassicadb.org/brad/>) using TopHat2 (version 2.1.1) [34]. Expression levels of genes were quantified with Cufflinks protocol [35], and transcript per million (TPM) values were used to determine expression levels.

### Cloning and bacterial expression of *BrFLS* genes

The coding sequences (CDSs) of *BrFLSs* were isolated from the cauline leaves of green Chinese cabbage by reverse transcription-PCR using antiRivert cDNA Synthesis Master mix (GenDEPOT, Barker, TX, USA), Q5 High-Fidelity DNA polymerase (New England Biolabs, Ipswich, MA, USA), and gene-specific primers (Supplementary Table S1). The CDSs were cloned into the pGEX-6P-1 vector and verified by sequencing, followed by their transformation into *Escherichia coli* BL21 (DE3) (Novagen, Darmstadt, Germany).

### Substrate-feeding assay of recombinant *BrFLS* proteins

Recombinant glutathione S-transferase (GST)-fused *BrFLS* proteins expression was induced by 100  $\mu$ M isopropyl  $\beta$ -D-1-thiogalactopyranoside (IPTG) at 20°C for 4 h. Small aliquots of the induced cultures were set aside for SDS-PAGE analysis. A total of 200  $\mu$ M of ( $\pm$ )-dihydrokaempferol (DHK) or ( $\pm$ )-naringenin (Nar) (Sigma-Aldrich, St. Louis, MO, USA) was added to the induced culture medium as a substrate. After 2 h incubation at 25°C, the culture medium was extracted with the same volume of ethyl acetate. The upper ethyl acetate phase was evaporated, and the resulting residue was recovered by dissolving in methanol and analyzed by high-performance liquid chromatography (HPLC) with a protocol previously described [36]. The production of protein was verified by SDS-PAGE.

### Transient expression of *BrFLS1* in *Nicotiana benthamiana* leaves

*BrFLS1* CDS was introduced into the binary vector pEarlyGate201 [37] via the Gateway cloning system to create a fusion construct containing N-terminal HA tag. Transformation of *Agrobacterium* GV3101 with the binary vector was carried out with the freeze-thaw method [38]. The transformed *Agrobacterium* was initially infiltrated into *N. benthamiana* leaves according to the previous method [36], and 4 days later, 100  $\mu$ M of ( $\pm$ )-Nar, ( $\pm$ )-DHK, or ( $\pm$ )-dihydroquercetin (DHQ) (Sigma-Aldrich) was infiltrated into the same leaves as a substrate, followed by incubation for 24 h. The leaf samples were extracted with 2 N HCl-containing 50% (v/v) methanol at 95°C for 2 h to convert flavonoid glycosides to aglycones and then analyzed by HPLC.

### Western blot analysis

Total protein of *N. benthamiana* leaves were extracted with an appropriate buffer (50 mM Tris-Cl (pH 8.0), 250 mM sucrose, 2 mM EDTA, 2 mM DTT, and 200  $\mu$ M phenylmethylsulfonyl fluoride). The supernatant separated through centrifugation (10 000  $\times$  g for 10 min) was used as a total protein, of which 20  $\mu$ g was applied for Western blot analysis with the anti-HA antibody according to the previous method [39].

### Construction of the CRISPR/Cas9 binary vector

Cas-Designer, a web-based guide RNA designing tool (<http://rgenome.net>) [40] was used to identify potential single-guide RNA

(sgRNA) sequences based on the genomic sequence of *BrFLS1*. Among them, three sequences (sg1, 5'-AGGGATGGCTTCGGTGTG-GA-3'; sg2, 5'-CCGGCGATCACCACCTTTCCG-3'; sg3, 5'-AACGTTCT-TCGAGCTTCCGT-3') next to the protospacer adjacent motif (PAM) sequences (5'-NGG-3') located within the first exon were selected, with expected out-of-frame scores of 68%, 60%, and 63%, respectively. DNA oligonucleotides of each sgRNA sequence were synthesized in the forward and reverse orientations and annealed by decreasing the temperature from 95°C to 25°C for 1.5 h. The resulting sgRNA DNA fragments were cloned into the binary vector pHAtC, according to a previously reported protocol [20]. The resulting CRISPR/Cas9 binary vector was introduced into *Agrobacterium* strain GV3101 by the freeze-thaw method.

### Chinese cabbage transformation

The Chinese cabbage transformation method was described previously [16]. The newly formed T<sub>0</sub> plants were transferred to soil after acclimatization and grown in a glasshouse for 4–5 days, vernalized at 4°C for ~45 days, and returned to the glasshouse. Genomic DNA of the cauline leaves from each T<sub>0</sub> plant was isolated and genotyped with PCR to detect the hygromycin resistance and *SpCas9* genes. After flowering, bud pollination of T<sub>0</sub> plant was conducted to obtain T<sub>1</sub> seeds. Genotyping of T<sub>1</sub> lines was conducted by PCR, and individual plants lacking the hygromycin resistance and *SpCas9* genes were selected and further analyzed by PCR and sequencing of the target site to verify editing of *BrFLS1*. The primers used for genotyping are listed in Supplementary Table S1.

### Off-target mutation analysis

Potential off-target edits of the sgRNAs were identified in the *B. rapa* genome using the CRISPR-GE web tool (<http://ski.scau.edu.cn>) [41]. BLAST hits containing potential off-target sequences that had fewer than four mismatches and were located in the coding sequence were selected (Supplementary Table S2). The sequences of other *BrFLS* genes corresponding to the target site were also considered as potential off-targets. PCR using specific primers (Supplementary Table S1) was performed to amplify the potential off-target sequences in the T<sub>1</sub> lines, and the products were analyzed by sequencing.

### Identification of flavonoid aglycones and glycosides

The leaf parts of the middle layers forming head of 75-day-old Chinese cabbages were sampled and lyophilized. Ground powder of the sample was extracted with 2 N HCl-containing 50% methanol at 95°C for 2 h for acid hydrolysis of flavonoids or with 70% (v/v) methanol for 30 min at 70°C for flavonoid glycosides extraction. The extracts were injected into a Shimadzu liquid chromatography (LC) system (Nexera X2 UHPLC) (Shimadzu) connected to a reversed-phase Shim-pack GIS-ODS-I column (3 μm, 3.0 × 100 mm) (Shimadzu). Water containing 0.1% (v/v) formic acid (Sol. A) and acetonitrile containing 0.1% (v/v) formic acid (Sol. B) were used as eluents with a flow rate of 0.5 mL·min<sup>-1</sup>. The temperature of column oven was maintained at 35°C, and the elution condition was optimized as follows: 0–1 min, 10% Sol. B; 1–25 min, 10%–100% Sol. B; 25–40 min, 100% Sol. B; 40–41 min, 10% sol. B (all v/v). Flavonoid aglycones and glycosides were analyzed by a quadrupole time-of-flight mass spectrometer (QTOF-MS) (TripleTOF™ 5600+, AB Sciex, Ontario, CA, USA) in electrospray ionization (ESI) modes. Peak extraction was performed by integration software (MasterView v1.1; AB Sciex). Mass spectrometry conditions were optimized as follows: curtain gas, 25 psi; heating

gas, 50 psi; nebulizing gas, 50 psi; ion spray voltage, floating between 4.5 and 5.5 kV; temperature, 550°C; fragmentation, 35 collision energy and 15 collision energy spread; scan range, 50–1500 m/z. K, Q, (±)-DHK, (±)-DHQ, IR, and Cya (Sigma-Aldrich) were used as standards for identification and quantification of flavonoid aglycones in samples.

### Total phenolic content measurement

The leaf part of the middle layer of 75-day-old Chinese cabbage was extracted with 80% methanol for 24 h at room temperature in darkness. The supernatant separated by centrifugation was mixed with the same volume of 0.5 N Folin & Ciocalteu's phenol reagent. After 5 min of incubation, 2.8 volume of 20% (w/v) Na<sub>2</sub>CO<sub>3</sub> was added to the mixture and incubated in darkness for 2 h. Absorbance of the mixture was measured at 760 nm, and the total phenolic content of the sample was calculated using gallic acid as a standard. The result was expressed in milligrams of gallic acid equivalents per gram of fresh weight (mg GAE·g<sup>-1</sup> FW).

### Quantitative PCR

Total RNAs were isolated from the leaf part of the middle layer of 75-day-old Chinese cabbage, and first-strand cDNA was synthesized as described above. The cDNA samples were diluted 3-fold and used for quantitative PCR (qPCR). The qPCR was conducted with AccuPower 2X GreenStar qPCR Master Mix (Bioneer, Daejeon, Republic of Korea) and primer sets (Supplementary Table S1). The PCR was performed with Bio-Rad CFX96 system (Bio-Rad Laboratories, CA, USA) under the following condition: 95°C for 5 min; 50 cycles at 95°C for 15 s; 58°C for 30 s. Reactions were carried out in triplicate, and data were normalized using *B. rapa* *Actin7* (*BrACT7*) as a housekeeping gene (Supplementary Table S1).

### Osmolytes treatment of Chinese cabbage

Nine-day-old seedlings of Chinese cabbage grown on solid MS medium containing 1% sucrose were transferred to the solid MS medium containing mannitol (200 mM or 400 μM) or NaCl (150 mM). After incubation for 6 days, their root lengths were measured, and their aerial parts were detached from the roots for chlorophyll content measurement with DMSO method described previously [42].

### Acknowledgements

This work was supported by the New Breeding Technologies Development Program [grant number PJ016545] of the Rural Development Administration, Republic of Korea.

### Author contributions

S.P. performed gene cloning, enzyme assay, HPLC, LC-ESI-QTOF-MS analysis, and wrote the manuscript. H.L. performed gene cloning, HPLC analysis, Chinese cabbage breeding, and off-target analysis. J.H., J.S., C.J.L., and J.O. contributed to the Chinese cabbage breeding, cultivation, and genotyping. S.H.L. analyzed the LC-ESI-QTOF-MS data. S.B.L., J.L., and S.L. performed data analysis and review. J.A.K. was in charge of Chinese cabbage transformation. B.K. designed and supervised this research and revised the final version of the manuscript.

### Data availability

All relevant data generated or analyzed are included in the manuscript or in supplementary materials.

## Conflict of interest statement

No conflict of interest declared.

## Supplementary Data

Supplementary data is available at *Horticulture Research* online.

## References

- Li Z, Lee HW, Liang X. et al. Profiling of phenolic compounds and antioxidant activity of 12 cruciferous vegetables. *Molecules*. 2018;**23**:1139
- Park CH, Yeo HJ, Park SY. et al. Comparative phytochemical analyses and metabolic profiling of different phenotypes of Chinese cabbage *Brassica rapa* ssp. *pekinensis*. *Foods*. 2019;**8**:587
- Owens DK, Alerding AB, Crosby KC. et al. Functional analysis of a predicted flavonol synthase gene family in *Arabidopsis*. *Plant Physiol*. 2008;**147**:1046–61
- Preuß A, Stracke R, Weisshaar B. et al. *Arabidopsis thaliana* expresses a second functional flavonol synthase. *FEBS Lett*. 2009;**583**:1981–6
- Schilbert HM, Schone M, Baier T. et al. Characterization of the *Brassica napus* flavonol synthase gene family reveals bifunctional flavonol synthases. *Front Plant Sci*. 2021;**12**:733762
- Cheng F, Wu J, Fang L. et al. Biased gene fractionation and dominant gene expression among the subgenomes of *Brassica rapa*. *PLoS One*. 2012;**7**:e36442
- Guo N, Cheng F, Wu J. et al. Anthocyanin biosynthetic genes in *Brassica rapa*. *BMC Genomics*. 2014;**15**:426
- Wang X, Wang H, Wang J. et al. The genome of the mesopolyploid crop species *Brassica rapa*. *Nat Genet*. 2011;**43**:1035–9
- He Q, Lu Q, He Y. et al. Dynamic changes of the anthocyanin biosynthesis mechanism during the development of heading Chinese cabbage *Brassica rapa* L. and *Arabidopsis* under the control of BrMYB2. *Front Plant Sci*. 2020a;**11**:593766
- Gao C. Genome engineering for crop improvement and future agriculture. *Cell*. 2021;**184**:1621–35
- Li J, Yu X, Zhang C. et al. The application of CRISPR/Cas technologies to *Brassica* crops: current progress and future perspectives. *αBIOTECH*. 2022;**3**:146–61
- Hong JK, Suh EJ, Park SR. et al. Multiplex CRISPR/Cas9 mutagenesis of BrVRN1 delays flowering time in Chinese cabbage *Brassica rapa* L. ssp. *pekinensis*. *Agriculture*. 2021;**11**:1286
- Su T, Wang W, Li P. et al. Natural variations of BrHISN2 provide a genetic basis for growth-flavour trade-off in different *Brassica rapa* subspecies. *New Phytol*. 2021;**231**:2186–99
- Xiong X, Liu W, Jiang J. et al. Efficient genome editing of *Brassica campestris* based on the CRISPR/Cas9 system. *Mol Gen Genomics*. 2019;**294**:1251–61
- Shin NR, Shin YH, Kim HS. et al. Function analysis of the PR55/B gene related to self-incompatibility in Chinese cabbage using CRISPR/Cas9. *Int J Mol Sci*. 2022;**23**:5062
- Kim NS, Yu J, Bae S. et al. Identification and characterization of PSEUDO-RESPONSE REGULATOR (PRR) 1a and 1b genes by CRISPR/Cas9-targeted mutagenesis in Chinese cabbage *Brassica rapa* L. *Int J Mol Sci*. 2022;**23**:6963
- Wellmann F, Lukacin R, Moriguchi T. et al. Functional expression and mutational analysis of flavonol synthase from *Citrus unshiu*. *Eur J Biochem*. 2002;**269**:4134–42
- Stracke R, de Vos RC, Bartelniewoehner L. et al. Metabolomic and genetic analyses of flavonol synthesis in *Arabidopsis thaliana* support the *in vivo* involvement of leucoanthocyanidin dioxygenase. *Planta*. 2009;**229**:427–45
- Chua CS, Biermann D, Goo KS. et al. Elucidation of active site residues of *Arabidopsis thaliana* flavonol synthase provides a molecular platform for engineering flavonols. *Phytochemistry*. 2008;**69**:66–75
- Kim H, Kim ST, Ryu J. et al. A simple, flexible and high-throughput cloning system for plant genome editing via CRISPR-Cas system. *J Integr Plant Biol*. 2016;**58**:705–12
- Falcone Ferreyra ML, Rius S, Emiliani J. et al. Cloning and characterization of a UV-B-inducible maize flavonol synthase. *Plant J*. 2010;**62**:77–91
- He Q, Wu J, Xue Y. et al. The novel gene BrMYB2, located on chromosome A07, with a short intron 1 controls the purple-head trait of Chinese cabbage *Brassica rapa* L. *Hortic Res*. 2020b;**7**:97
- Yin R, Messner B, Faus-Kessler T. et al. Feedback inhibition of the general phenylpropanoid and flavonol biosynthetic pathways upon a compromised flavonol-3-O-glycosylation. *J Exp Bot*. 2012;**63**:2465–78
- Auger B, Marnet N, Gautier V. et al. A detailed survey of seed coat flavonoids in developing seeds of *Brassica napus* L. *J Agric Food Chem*. 2010;**58**:6246–56
- Hald C, Dawid C, Tressel R. et al. Kaempferol 3-O-2-O-Sinapoyl-beta-sophoroside causes the undesired bitter taste of canola/rapeseed protein isolates. *J Agric Food Chem*. 2019;**67**:372–8
- Wen J, Zhu L, Qi L. et al. Characterization of interloid hybrids from crosses between *Brassica juncea* and *B. Oleracea* and the production of yellow-seeded *B. Napus*. *Theoretical and Applied Genetic*. 2012;**125**:19–32
- Jiang J, Shao Y, Li A. et al. Phenolic composition analysis and gene expression in developing seeds of yellow- and black-seeded *Brassica napus*. *J Integr Plant Biol*. 2013;**55**:537–51
- Zhang XF, Hung TM, Phuong PT. et al. Anti-inflammatory activity of flavonoids from *Populus davidiana*. *Arch Pharm Res*. 2006;**29**:1102–8
- Zhang WY, Lee JJ, Kim IS. et al. Stimulation of glucose uptake and improvement of insulin resistance by aromadendrin. *Pharmacology*. 2011;**88**:266–74
- Zhang Y, Yan G, Sun C. et al. Apoptosis effects of dihydrokaempferol isolated from *Bauhinia championii* on synovial cells. *Evid Based Complement Alternat Med*. 2018;**2018**:9806160
- Zhang Y, Zhang D, Tang Y. et al. Aromadendrin: a dual amyloid promoter to accelerate fibrillization and reduce cytotoxicity of both amyloid- $\beta$  and hIAPP. *Materials Advances*. 2020;**1**:1241–52
- Lee HS, Jeong GS. Aromadendrin inhibits T cell activation via regulation of calcium influx and NFAT activity. *Molecules*. 2020;**25**:4590
- Lee HS, Kim EN, Jeong GS. Aromadendrin protects neuronal cells from methamphetamine-induced neurotoxicity by regulating endoplasmic reticulum stress and PI3K/Akt/mTOR signaling pathway. *Int J Mol Sci*. 2021;**22**:2274
- Kim D, Perteau G, Trapnell C. et al. TopHat2: accurate alignment of transcriptomes in the presence of insertions, deletions and gene fusions. *Genome Biol*. 2013;**14**:R36
- Trapnell C, Williams BA, Pertea G. et al. Transcript assembly and quantification by RNA-Seq reveals unannotated transcripts and isoform switching during cell differentiation. *Nat Biotechnol*. 2010;**28**:511–5
- Park S, Lee H, Min MK. et al. Functional characterization of BrF3'H, which determines the typical flavonoid profile of purple Chinese cabbage. *Front Plant Sci*. 2021;**12**:793589

37. Earley KW, Haag JR, Pontes O. *et al.* Gateway-compatible vectors for plant functional genomics and proteomics. *Plant J.* 2006;**45**: 616–29
38. Holsters M, de Waele D, Depicker A. *et al.* Transfection and transformation of *Agrobacterium tumefaciens*. *Mol Gen Genomics.* 1978;**163**:181–7
39. Park S, Choi MJ, Lee JY. *et al.* Molecular and biochemical analysis of two rice flavonoid 3'-hydroxylase to evaluate their roles in flavonoid biosynthesis in rice grain. *Int J Mol Sci.* 2016;**17**:1549
40. Bae S, Kweon J, Kim HS. *et al.* Microhomology-based choice of Cas9 nuclease target sites. *Nat Methods.* 2014;**11**:705–6
41. Xie X, Ma X, Zhu Q. *et al.* CRISPR-GE: a convenient software toolkit for CRISPR-based genome editing. *Mol Plant.* 2017;**10**: 1246–9
42. Manolopoulou E, Varzakas TH, Petsalaki A. Chlorophyll determination in green pepper using two different extraction methods. *Current research in nutrition and food science.* 2016;**4**: 52–60